

BBA 71200

## INVESTIGATION OF HUMAN ERYTHROCYTE GHOST MEMBRANES WITH INTRAMOLECULAR EXCIMER PROBES

KLAAS A. ZACHARIASSE, WINCHIL L.C. VAZ, CARLOS SOTOMAYOR \*,  
and WOLFGANG KÜHNLE

*Max-Planck-Institut für biophysikalische Chemie, Am Fassberg, Postfach 968, D-3400 Göttingen (F.R.G.)*

(Received October 2nd, 1981)

*Key words: Pyrene probe; Fluorescence; Membrane structure; (Human erythrocyte)*

Human erythrocyte ghost membranes have been investigated using two intramolecular excimer probes, di(1-pyrenyl)propane and di(1-pyrenylmethyl) ether. Values for the viscosity of the direct probe environment in the ghost membranes range from 76 cP at 37°C to 570 cP at 5°C, as reported for di(1-pyrenyl)propane, with liquid paraffin as the reference solvent. For the activation energy of the excimer formation process, determined here mainly by the viscosity of the medium, a value of 37 kJ/mol is obtained. The other probe molecule reports a higher local viscosity, 133 cP at 37°C, as well as a higher activation energy of excimer formation, 54 kJ/mol. Neither thermotropic phase transitions nor temperature hysteresis effects are observed within the temperature range (0 to 40°C) studied. From the vibrational structure of the fluorescence spectrum of di(1-pyrenylmethyl) ether, a polarity of the probe environment close to that of hexanol ( $\epsilon = 13.3$ ) results for the erythrocyte ghost membranes. The polarity measured in egg phosphatidylcholine membranes and in multibilayers of dimyristoylphosphatidylcholine is slightly larger, comparable to that of butanol ( $\epsilon = 17.5$ ), whereas a polarity comparable to that of methanol ( $\epsilon = 32.7$ ) is observed for aqueous micellar solutions of sodium dodecyl sulphate. Further, from the wavelength shifts in the absorption spectrum of di(1-pyrenyl)propane and di(1-pyrenylmethyl) ether, the polarizability of the probe surroundings can be determined, leading to a surprisingly high value for the apparent refractive index. This is attributed to a high local density of the direct environment of the probe, for which a location between the membrane/water interface and the unpolar bilayer mid-plane is deduced.

### Introduction

Intramolecular excimer probes consisting of pyrenes linked together by either a trimethylene [1,2] or a dimethyl ether [3] chain, have been employed to investigate their direct environment

in micelles [1] and synthetic phospholipid bilayers [2,3]. The advantage of intramolecular over intermolecular [4,5] excimer probes lies primarily in the possibility the former offer to use the probe molecule in very small concentrations,  $1 \cdot 10^{-6}$  M and lower [1,2]. This minimizes (but see Ref. 2) the perturbation of the medium under investigation and avoids the formation of probe aggregates, a phenomenon that has been encountered with pyrene [4].

In the present paper, intramolecular excimer formation in human erythrocyte ghost membranes and in other systems is reported for two probe

\* Present address: Universidad Catolica de Valparaiso, Av. Brasil 2950, Casilla 4059, Valparaiso, Chile.

Abbreviations: PC, phosphatidylcholine; DMPC, dimyristoylphosphatidylcholine;  $\text{Py}(\text{CH}_2)_3\text{Py}$ , 1,3-di(1-pyrenyl)propane;  $\text{PyCH}_2\text{OCH}_3$ , (1-pyrenylmethyl)methyl ether;  $\text{PyCH}_2\text{OCH}_2\text{Py}$ , di(1-pyrenylmethyl) ether; SDS, sodium dodecyl sulphate.

molecules, 1,3-di(1-pyrenyl)propane ( $\text{Py}(\text{CH}_2)_3\text{Py}$ ) and di(1-pyrenylmethyl) ether ( $\text{PyCH}_2\text{OCH}_2\text{Py}$ ), differing in the molecular nature of the chain connecting the pyrenes. This variation can in principle lead to different mean solubilization sites for the two probe molecules.

Erythrocyte ghost membranes were taken as the medium to be investigated. The human erythrocyte membrane is one of the best studied biological membranes. The ready accessibility, ease of preparation and wealth of available information make this membrane a useful system for the evaluation of new probes in biological membrane systems. Erythrocyte membranes have been studied using a large variety of techniques apart from fluorescence [6–9], such as electron spin resonance [10,11], nuclear magnetic resonance [6,12], Raman spectroscopy [13], X-ray diffraction [14] and viscometry [15].

Fluidity of biological membranes, the term is used here in a purely operational manner [1], may control several important processes occurring in these membranes [16]. Investigations using time-resolved fluorescence anisotropy decay measurements with diphenylhexatriene solubilized in erythrocyte membranes indicate these to have an apparent viscosity of 141 and 57 cP, at 5 and 37°C, respectively [7].

Some controversy exists regarding the thermotropic behaviour of the erythrocyte membrane, i.e., the occurrence of phase transitions [8,13,15,17] and the meaning of the hysteresis in the temperature dependence of the membrane fluidity which was observed by some authors [8]. The early viscometric study of Zimmer and Schirmer [15], suggesting a thermotropic phase transition at about 18°C in the intact membrane, has been corroborated by some authors [8,10,13,17] but was contradicted by others [6,11,12,14].

The excimer-to-monomer fluorescence quantum yield ratio,  $\phi'/\phi$ , can be expressed by Eqn. 1 [18,2], provided that any perturbation of the kinetics due to the chain connecting the two end-groups can be neglected.

$$\frac{\phi'}{\phi} = \frac{k'_f}{k_f} \frac{k_a}{k_d + 1/\tau'_0} \quad (1)$$

Here  $k'_f$ ,  $k_f$ ,  $k_a$  and  $k_d$  are the rate constants of

excimer fluorescence, monomer fluorescence, excimer association and dissociation, respectively, and  $\tau'_0$  is the excimer lifetime. For systems in the low-temperature region [2], i.e., when  $k_d \ll 1/\tau'_0$ , Eqn. 1 reduces to

$$\frac{\phi'}{\phi} = \frac{k'_f}{k_f} k_a \tau'_0 \quad (2)$$

These conditions were found to hold for the erythrocyte ghost membranes over the temperature range considered here (0 to 40°C). This being the case, the temperature dependence of the excimer-to-monomer fluorescence intensity ratio  $I'/I$ , being directly proportional to  $\phi'/\phi$ , is determined primarily by the rate constant of excimer formation,  $k_a$  [2].

Intramolecular excimer formation in viscous media such as phospholipid bilayers, is mainly determined by the movement of the end-groups through the medium, i.e., by the fluidity of the environment, and not by constraints resulting from rotations of the chain, which involve considerably smaller activation energies [19]. A study of intramolecular excimer fluorescence, giving values of  $I'/I$ , as a function of temperature, can therefore give information on the nature of a medium, in so far as this affects intramolecular excimer formation, i.e., on the fluidity [1,2].

## Experimental

The erythrocyte ghosts were prepared from outdated blood (Universitätsklinik Göttingen) following the method of Dodge et al. [20]. The ghosts were frozen quickly to  $-70^\circ\text{C}$  and stored at this temperature until further use. For incorporation of the probes, the ghosts were rapidly thawed, suspended in 10 mM potassium phosphate (pH 7.4)/100 mM KCl to a concentration of 1 mg protein/ml. A solution of the probes in ethanol ( $1 \cdot 10^{-4}$  M) was injected into the ghost suspension while gently vortexing. The probe-to-erythrocyte total lipid molar ratio was smaller than 0.001. The suspension was then shaken at  $4^\circ\text{C}$  for 12 h before the fluorescence measurements were made. This method resulted in reproducible incorporation of the probes into the membranes. Depositing the probe as a film on the wall of a container and

subsequent prolonged shaking or vortexing of the aqueous ghost suspension, a successful method with phosphatidylcholine bilayers [2] and chromaffin granules (Morris, S.J. and Zachariasse, K.A., unpublished data), did not lead to sufficient solubilization of the probes into the ghost membranes. For multilamellar liposomes of dimyristoylphosphatidylcholine (DMPC) both methods of probe incorporation gave identical results. The nature of the solvent used for the former procedure is important, however. Introduction of the probe as a solution in tetrahydrofuran of similar concentration and volume as in the case of ethanol, resulted in higher excimer-to-monomer fluorescence intensity ratios than those found when an ethanolic solution was used. This may be due to preferential solvation of the probe molecules by tetrahydrofuran, which solvent tends to form complexes with aromatic hydrocarbons [21].

Fluorescence measurements at 4°C, as a function of time after probe injection, showed that the excimer-to-monomer fluorescence intensity ratio reaches a constant (minimum) value after approx. 6 h. The initially higher value of  $I'/I$  may be caused by the fact that both dipyranyl compounds employed here as probe molecules are only very slightly soluble (less than  $1 \cdot 10^{-7}$  M) in water and may thus tend to form aggregates in aqueous solution. Control experiments in which the probe molecules were injected into aqueous buffers which did not contain erythrocyte ghosts, showed only excimer fluorescence. The incorporation time of 6 h then reflects the time necessary for the complete transfer of the probe molecule from the aqueous phase into the membranes.

The fluorescence spectra of the erythrocyte ghost suspensions were run from 0 to 38°C. All preparations were measured within 24 h after preparation. Oxygen was removed by bubbling pure nitrogen through the suspensions for 15 min prior to the fluorescence measurements. For each preparation containing a probe molecule, an equivalent preparation without the probe was measured under identical conditions, to subtract the background due to light scattering. Also a correction was made for the contribution of the monomer fluorescence at the wavelength where the excimer fluorescence intensity,  $I'$ , was determined.

1,3-Di(1-pyrenyl)propane and di(1-pyrenyl-

methyl) ether were synthesized using methods described before [22,3]. (1-Pyrenylmethyl)methyl ether,  $\text{PyCH}_2\text{OCH}_3$ , was synthesized from 1-pyrenylmethanol and methyl iodide using the same procedure as adopted for the dipyranyl ether [24]. The fluorescence measurements were carried out on a Hitachi-Perkin Elmer MPF-2 fluorimeter. The absorption spectra were run on a Cary 17, equipped with a thermostatically controlled cell compartment.

The following solvents have been used (Uvasol (Merck) or the best commercially available, quality): (1) methanol; (2) acetonitrile; (3) acetone; (4) ethanol; (5) diisopropyl ether; (6) *n*-hexane; (7) 1-propanol; (8) 1-butanol; (9) dibutyl ether; (10) 1-pentanol; (11) 1-hexanol; (12) methylcyclohexane; (13) dioxane; (14) ethylene glycol; (15) *n*-hexadecane; (16) 1,3-propanediol; (17) dimethyl sulphoxide; (18) liquid paraffin; (19) toluene; (20) pyridine; (21) chlorobenzene; (22) benzonitrile; and (23) glycerol. The dielectric constants  $\epsilon$  refer to 25°C.

Dimyristoylphosphatidylcholine was purchased from Fluka and egg phosphatidylcholine was obtained from fresh egg yolks according to the method of Singleton et al. [24]. SDS was recrystallized three times from ethanol.

## Results and Discussion

### (A) Spectral data

Fluorescence spectra of  $\text{Py}(\text{CH}_2)_3\text{Py}$  as well as of  $\text{PyCH}_2\text{OCH}_2\text{Py}$  solubilized in aqueous erythrocyte ghost suspensions show, besides the monomer fluorescence component, a contribution originating from the intramolecular excimer (see Fig. 1). The excimer-to-monomer fluorescence intensity ratio  $I'/I$ , where  $I'$  and  $I$  are measured at 500 nm and at 379 or 398 nm, respectively, increases strongly with temperature for both probe molecules, as is shown in Fig. 2. The results are independent of the direction of the temperature scan, i.e., no hysteresis in the temperature measurements is detected, below 40°C (see Ref. 8). Neither are any phase transitions observed, in contrast to earlier reports using various techniques [8,10,13,15,17] (see above). It is of interest to note here that both dipyranyl probes readily detect the main phase transitions [2,3] and the pretransitions

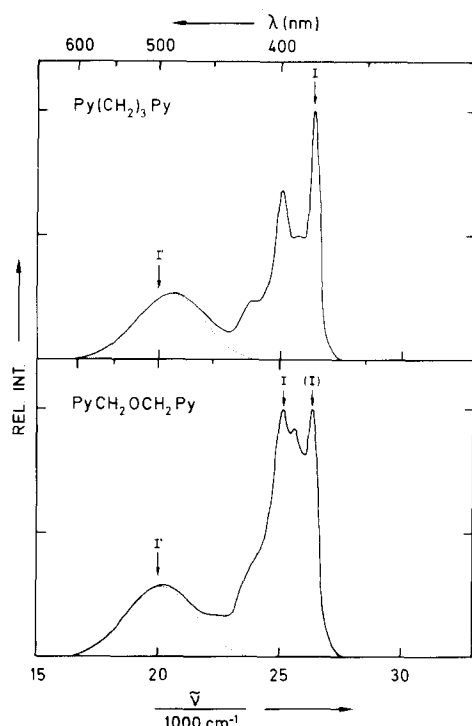


Fig. 1. Fluorescence spectra of di(1-pyrenyl)propane ( $\text{Py}(\text{CH}_2)_3\text{Py}$ ), above, and di(1-pyrenylmethyl) ether ( $\text{PyCH}_2\text{OCH}_2\text{Py}$ ), below, in aqueous suspensions of erythrocyte ghost membranes, at  $37^\circ\text{C}$ . The arrows indicate the monomer ( $I$ ) and excimer ( $I'$ ) fluorescence intensities. For  $\text{PyCH}_2\text{OCH}_2\text{Py}$  the monomer fluorescence intensity is determined at two wavelengths,  $I$  at 398 nm and ( $I$ ) at 379 nm. See Table I and text. The (partially dotted) excimer emission bands with a maximum around  $20000\text{ cm}^{-1}$  have been obtained by subtracting the monomer spectra from the total fluorescence spectra.

[2] in multibilayer dispersions and sonicated vesicles of phosphatidylcholines.

In the low-temperature limit of excimer formation, where, as discussed above, Eqn. 2 holds, a plot of  $\ln I'/I$  vs. the reciprocal absolute temperature gives a straight line with the activation energy,  $E_a$ , of the excimer formation process as the slope (see Fig. 2). It is clear that for both probe molecules the low-temperature limit holds over the entire temperature range investigated here. The two probes give different values for  $E_a$ , 37 kJ/mol for  $\text{Py}(\text{CH}_2)_3\text{Py}$ , as compared to 54 kJ/mol for  $\text{PyCH}_2\text{OCH}_2\text{Py}$ , whereas for liquid paraffin identical values, 45 and 47 kJ/mol respectively, are found. These results signify that the direct en-

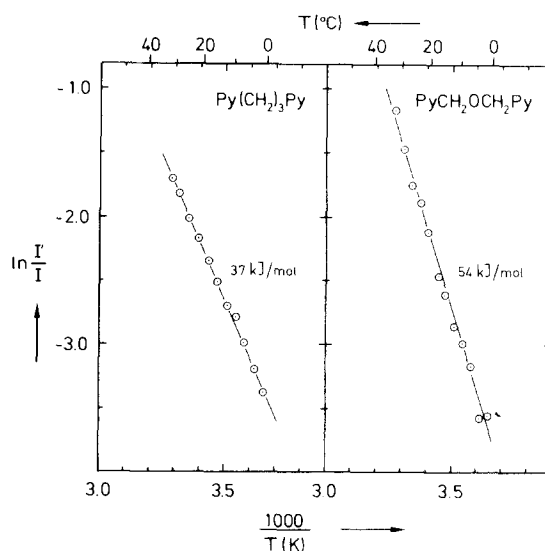


Fig. 2. The logarithm, of the excimer-to-monomer fluorescence intensity ratio,  $I'/I$ , in erythrocyte ghost membranes, as a function of the reciprocal absolute temperature  $T$  (K), for  $\text{Py}(\text{CH}_2)_3\text{Py}$  (left) and  $\text{PyCH}_2\text{OCH}_2\text{Py}$  (right).  $I'$  is measured at 500 nm, whereas  $I$  is determined at 379 nm and at both 379 and 398 nm for  $\text{Py}(\text{CH}_2)_3\text{Py}$  and  $\text{PyCH}_2\text{OCH}_2\text{Py}$ , respectively (see Table I). The activation energies of the intramolecular excimer association process, determined from the slopes of the lines, are indicated in the figure.  $1\text{ kcal} = 4.184\text{ kJ}$ .

vironment of  $\text{Py}(\text{CH}_2)_3\text{Py}$  in the erythrocyte ghosts is different from that of  $\text{PyCH}_2\text{OCH}_2\text{Py}$ , suggesting a lower viscosity in the former case, see below.

An alternative interpretation that the different apparent viscosity obtained with the two probe molecules reflects a difference in the probe motion, affecting the rate constant of excimer formation,  $k_a$ , and hence the values of  $E_a$  and of the measured fluidity, cannot be excluded a priori. This interpretation does not appear to be plausible, however, as in liquid paraffin practically identical values for  $E_a$  were observed, see above.

#### (B) Erythrocyte membrane viscosity

The excimer-to-monomer fluorescence intensity ratio,  $I'/I$ , of the probe molecules in the erythrocyte ghost membrane can be translated into viscosity values by comparing this intensity ratio with those measured in an appropriate solvent or solvent mixture of known macroscopic viscosity. For this purpose, liquid paraffin was chosen as the solvent. However, with  $\text{Py}(\text{CH}_2)_3\text{Py}$  as well as with

$\text{PyCH}_2\text{OCH}_2\text{Py}$ , the  $I'/I$  values for the erythrocyte membranes and for the other membrane systems were found to be lower than those in liquid paraffin. Attempts to use ethylene glycol/glycerol mixtures to obtain model solvent viscosities more directly comparable with those of the membrane systems were unsuccessful since the fluorescence spectra of the probes showed aggregate formation in mixtures with large percentages of glycerol. The viscosity values for the erythrocyte ghost membranes were therefore determined by extrapolation of the liquid paraffin data, using a plot of  $I'/I$  versus the reciprocal macroscopic viscosity  $\eta$ . The  $I'/I$  value obtained with the probe molecule in liquid paraffin at a given temperature (and therefore viscosity) was linearly extrapolated to  $1/\eta = 0$ , where  $I'/I = 0$  (see Eqn. 1). The, lower,  $I'/I$  value measured at the same temperature in, for example, the erythrocyte ghost membrane then graphically corresponds to a value for  $1/\eta$ , giving the membrane viscosity that is based, in this procedure, on liquid paraffin.

The value of 76 cP for the apparent viscosity of the erythrocyte ghosts at 37°C, determined with  $\text{Py}(\text{CH}_2)_3\text{Py}$  using the procedure outlined above, compared reasonably well with the value of 57 cP deduced by Glatz [7]. Our value at 5°C, 570 cP, is considerably higher than that found by Glatz, 141 cP, however,

The viscosity values obtained for the erythrocyte ghost membranes with  $\text{Py}(\text{CH}_2)_3\text{Py}$  have been plotted as a function of temperature in Fig. 3. A logarithmic plot of these data versus the reciprocal absolute temperature results in a non-linear relationship, the slope changing from 41 to 51 kJ/mol at the upper and lower temperatures, respectively. This is not too surprising, as also for liquid paraffin, the reference solvent, such a plot is nonlinear, due to the fact that this solvent contains alkane molecules with a non-uniform chain-length distribution.

For the other probe molecule,  $\text{PyCH}_2\text{OCH}_2\text{Py}$ , using the same extrapolation procedure, considerably higher values for the local viscosity in erythrocyte ghost membranes result: from 133 cP at 37°C to 1550 cP at 5°C (see Table I and below). A similar difference was observed for the activation energies of excimer formation  $E_a$ , see above. The difference in ghost viscosity reported by the

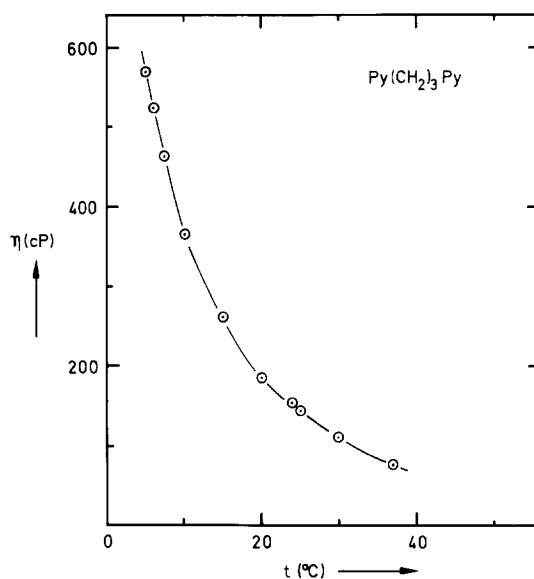


Fig. 3. The temperature dependence of the apparent viscosity of the direct environment of the probe molecule  $\text{Py}(\text{CH}_2)_3\text{Py}$  in erythrocyte ghost membranes, using liquid paraffin as the reference solvent. See text.

two probes can reflect a difference in the mean distribution of the solubilized probe molecule over the membrane. For synthetic phosphatidylcholines it has been reported that the bilayer is less fluid close to the bilayer/water interface than it is towards the interior [25,26]. If this is also the case for the erythrocyte ghost membrane, then the  $\text{PyCH}_2\text{OCH}_2\text{Py}$  molecule would appear to be solubilized closer to the membrane/water interface than is  $\text{Py}(\text{CH}_2)_3\text{Py}$ .

A word of caution is in order as to the exact meaning of these viscosity data, as the values are only as good as the extent to which the reference solvent is a good model for the particular environment. It may be impossible to find a homogeneous solvent that can truthfully represent the nature of the local environment in intrinsically inhomogeneous and anisotropic systems such as biological membranes. This exposes the limits inherent in the use of probe molecules, which moreover have molecular dimensions that cannot be ignored and which always more-or-less perturb their environment. Nevertheless, useful information can be extracted from studies based on probe molecules. Probe molecules often find their optimal applica-

TABLE I

VISCOSITIES (IN cP) DERIVED FROM EXCIMER-TO-MONOMER FLUORESCENCE INTENSITY RATIOS FOR DI(1-PYRENYL)PROPANE ( $\text{Py}(\text{CH}_2)_3\text{Py}$ ) AND DI(1-PYRENYLMETHYL) ETHER ( $\text{PyCH}_2\text{OCH}_2\text{Py}$ ) IN VARIOUS MEDIA AT 37°C

Values are viscosities taken with liquid paraffin as the reference solvent, having a viscosity of 47 cP at 37°C. The viscosity data derived from  $\text{PyCH}_2\text{OCH}_2\text{Py}$  are less meaningful than the data based on  $\text{Py}(\text{CH}_2)_3\text{Py}$ , because of the solvent polarity dependence of the monomer fluorescence spectrum of  $\text{PyCH}_2\text{OCH}_2\text{Py}$ . The fluorescence intensity of the excimer emission  $I'$  has been determined at 500 nm for both probe molecules, whereas the monomer fluorescence intensity  $I$  was measured at 379 nm for  $\text{Py}(\text{CH}_2)_3\text{Py}$  and at 398 nm for  $\text{PyCH}_2\text{OCH}_2\text{Py}$ . With the latter probe molecule the value in parentheses refers to 379 nm. These last values suffer more strongly from the solvent influence on the monomer fluorescence spectrum than the values based on the intensity determination at 398 nm. See text.

	$\text{Py}(\text{CH}_2)_3\text{Py}$	$\text{PyCH}_2\text{OCH}_2\text{Py}$
Erythrocyte ghosts	76	133 (200)
DMPC multilamellar liposomes	23	53 (80)
EGG PC multilamellar liposomes	—	69 (110)
0.1 M SDS micellar solution	12	20 (50)

tion not so much in experiments designed to give absolute values for some physical property, but rather in investigations of differences between structurally related media or of changes taking place in a particular system, such as, for instance, those due to variations in temperature. It seems that the results of a variety of different probe molecules will have to be collated and combined with the results of other methods of investigation to obtain a more detailed picture of any inhomogeneous environment.

### (C) Conclusions on probe location

An important question when using probe molecules concerns the determination of their location in a medium. With the probes employed here the fluorescence and absorption spectra contain information which can be used to investigate this problem.

*1. Vibrational structure of the fluorescence spectra.* The vibrational structure of the monomer fluorescence spectrum of one of the probe molecules,  $\text{PyCH}_2\text{OCH}_2\text{Py}$  (see Fig. 1), and also of the related molecule,  $\text{PyCH}_2\text{OCH}_3$ , depends on the nature of the solvent. This phenomenon, the Ham effect [27,28], has been observed before with unsubstituted aromatic hydrocarbons such as pyrene, naphthalene and benzene. As in the case of pyrene, the zero-zero vibrational peak in the fluorescence spectrum of  $\text{PyCH}_2\text{OCH}_2\text{Py}$  and  $\text{PyCH}_2\text{OCH}_3$  increases in intensity with respect to the other peaks as the solvent polarity increases. For the other dipyranyl compound,  $\text{Py}(\text{CH}_2)_3\text{Py}$ , only a weak Ham effect is observed, as in the case of 1-methylpyrene.

The intensity ratio of the fluorescence peaks of  $\text{PyCH}_2\text{OCH}_2\text{Py}$  at 379 and 390 nm,  $I_{379}/I_{390}$ , is plotted as a function of solvent polarity, characterized by the polarity-polarizability parameter  $f - \frac{1}{2}f'$  [29] (see Fig. 4). Here  $f = (\epsilon - 1)/(2\epsilon + 1)$ , the dielectric constant function, and  $f' = (n^2 - 1)/(2n^2 + 1)$ , the refractive index function. It is seen from Fig. 4 that a correlation exists between the fluorescence intensity ratio  $I_{379}/I_{390}$  and the solvent polarity parameter  $f - \frac{1}{2}f'$ . The highest values for this ratio are observed for highly polar solvents such as dimethyl sulphoxide (No. 17), glycerol (No. 23) and methanol (No. 1). Similar plots are obtained employing other solvent polarity scales, such as the well-known  $E_T(30)$  [30].

The fluorescence intensity ratios observed with  $\text{PyCH}_2\text{OCH}_2\text{Py}$  solubilized in erythrocyte ghosts (E. Ghosts), egg phosphatidylcholine (egg PC) and dimyristoylphosphatidylcholine (DMPC) and in aqueous micellar solutions of SDS have been indicated as line segments in Fig. 4. The  $I_{379}/I_{390}$  ratio for the erythrocyte ghosts is the lowest of these four media, with a value close to that of 1-hexanol ( $\epsilon = 13.3$ , No. 11). A larger value for  $I_{379}/I_{390}$  is observed for egg PC and multibilayers of DMPC, corresponding to 1-butanol ( $\epsilon = 17.5$ , No. 8). The largest  $I_{379}/I_{390}$  ratio is observed in the SDS micelles, with a value between that of methanol ( $\epsilon = 32.7$ , No. 1) and ethanol ( $\epsilon = 24.6$ , No. 4). These results signify that in SDS the  $\text{PyCH}_2\text{OCH}_2\text{Py}$  probe molecule is solubilized close to the aqueous micellar surface, whereas it is solubilized further away from the aqueous interface in egg PC

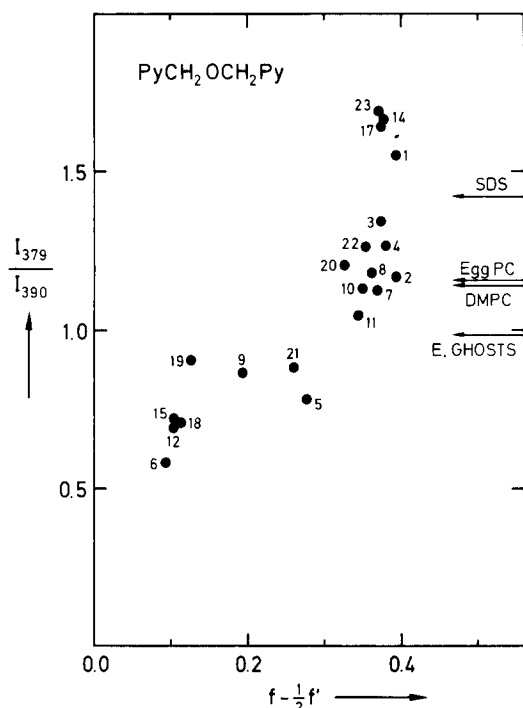


Fig. 4. The ratio of the fluorescence intensities at 379 and 390 nm,  $I_{379}/I_{390}$ , determined at the peaks in the spectrum of  $\text{PyCH}_2\text{OCH}_2\text{Py}$  at  $30^\circ\text{C}$ , as a function of the solvent polarity parameter  $f - \frac{1}{2}f'$  (see text). The  $I_{379}/I_{390}$  ratios observed with the probe molecule solubilized in a 0.1 M aqueous micellar solution of SDS and in membrane systems of egg PC, DMPC and erythrocyte ghosts (E. Ghosts), are indicated by line segments. For the numbers of the solvents, see Experimental.

and DMPC bilayers, and even further in the case of the erythrocyte ghosts. Still, the probe surroundings are far removed from being a purely alkane-chain environment such as hexadecane (No. 15). With  $\text{PyCH}_2\text{OCH}_3$  a similar plot of  $I_{379}/I_{390}$  vs.  $f - \frac{1}{2}f'$  is obtained. However, with this probe molecular the  $I_{379}/I_{390}$  ratio in erythrocyte ghosts has the same value as for egg PC and DMPC, comparable to 1-butanol. This means that the  $\text{PyCH}_2\text{OCH}_3$  probe molecule does not penetrate as far into the erythrocyte membrane as does  $\text{PyCH}_2\text{OCH}_2\text{Py}$ .

As shown above, the specific molecular properties of a solvent, mainly the polarity, determine the peak distribution in the fluorescence spectrum of  $\text{PyCH}_2\text{OCH}_2\text{Py}$ , to a much greater extent than in the case of  $\text{Py}(\text{CH}_2)_3\text{Py}$ . For this reason, the latter probe molecule is better suited for viscosity mea-

surements in unknown media, for which the  $I'/I$  ratios in such media are compared with those in model solvents, as was described above. Any difference in polarity between the medium and the model solvent would lead to different intensity ratios of the vibrational peaks in the monomer fluorescence spectrum of  $\text{PyCH}_2\text{OCH}_2\text{Py}$  and therefore to different  $I'/I$  ratios having no direct connection to macroscopic viscosity.

**2. Absorption spectra.** The absorption spectra of both probe molecules  $\text{Py}(\text{CH}_2)_3\text{Py}$  and  $\text{PyCH}_2\text{OCH}_2\text{Py}$  are similar to that of 1-ethylpyrene or 1-methylpyrene. The first absorption band (see Fig. 5) is only weakly allowed,  $^1\text{L}_b$  in the Platt notation [31], whereas the second absorption band,  $^1\text{L}_a$  [31,32], has a much larger transition dipole moment. The absorption spectra of dissolved molecules are generally affected by the nature of the solvent. As has already been known for more than a century [33,34], the spectral position of an absorption band responds mainly to the polarizability of the medium, i.e., to the refractive index,  $n$ , and not so much to other solvent properties such as the dielectric constant,  $\epsilon$ .

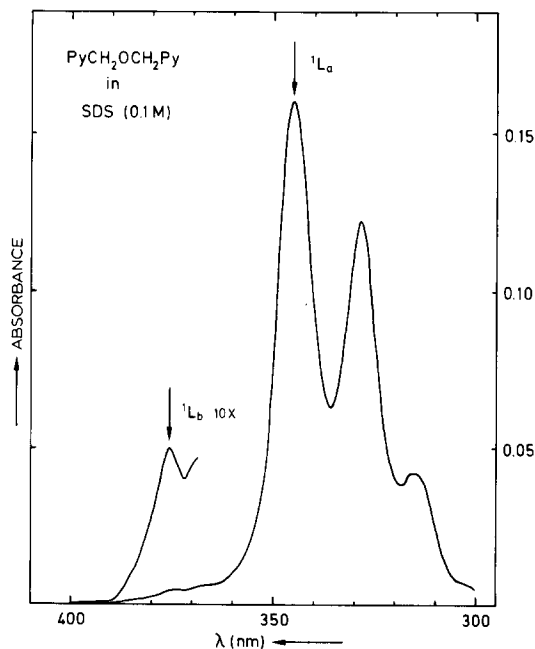


Fig. 5. Absorption spectrum of  $\text{PyCH}_2\text{OCH}_2\text{Py}$  in a 0.1 M aqueous micellar solution of SDS at  $20^\circ\text{C}$ . The first absorption peaks of the two lowest energy transitions in the absorption spectrum,  $^1\text{L}_b$  and  $^1\text{L}_a$  (see text), are indicated with arrows.

The spectral shift,  $\Delta\nu$ , due to the solvent polarizability, i.e., due to the London dispersion forces, can be expressed as [35]

$$\Delta\nu = 10.71 \cdot 10^9 \frac{f}{\nu a^3} \cdot \frac{n^2 - 1}{2n^2 + 1} \quad (3)$$

where  $f$  is the oscillator strength of the absorption band at the transition energy  $\nu$  (in  $\text{cm}^{-1}$ ), and  $a$  (in Å) stands for the radius of the spherical solvent cavity that had to be created to accommodate the solute molecule. The oscillator strength,  $f$ , is a direct measure of the intensity of a band in the absorption spectrum. It is therefore clear from Eqn. 3 that the effect of solvent polarizability, expressed by  $(n^2 - 1)/(2n^2 + 1)$ , will be much stronger for allowed absorption bands, such as the  $^1L_a$  band in Fig. 5, than for bands such as the  $^1L_b$  having a much smaller value for the oscillator strength. For instance, the energy of the first absorption peak of the  $^1L_a$  band of 1-ethylpyrene, is blue-shifted in a polar solvent of low refractive index ( $n = 1.3298$ ) such as methanol (340.8 nm) with respect to a nonpolar solvent of higher refractive index ( $n = 1.4120$ ) such as decane (342.6 nm). Therefore, the spectral position of the first strong absorption peak ( $^1L_a$ ) of the probe molecules  $\text{Py}(\text{CH}_2)_3\text{Py}$  and  $\text{PyCH}_2\text{OCH}_2\text{Py}$  contains information on the molecular nature, in this case on the polarizability, of their direct surroundings.

In order to obtain this information, the energy of the first vibrational peak of the  $^1L_a$  band in the absorption spectrum of  $\text{PyCH}_2\text{OCH}_2\text{Py}$ , indicated in Fig. 5, has been measured in a number of solvents. The results are plotted in Fig. 6, as a function of the polarizability parameter  $(n^2 - 1)/(2n^2 + 1)$ , see Eqn. 3, showing a good linear correlation. When the data are plotted as a function of the dielectric constant or of the solvent polarity parameters  $E_T(30)$  or  $f - \frac{1}{2}f'$  (see above), no such correlation between the data and the solvent parameter is observed. Also indicated in Fig. 6, as line segments, are the absorption peak energies of  $\text{PyCH}_2\text{OCH}_2\text{Py}$  in the three membrane systems, erythrocyte ghosts, DMPC and egg PC, and in an anionic micellar solution of SDS.

The apparent polarizability, i.e., refractive index  $n$ , of the direct environment of  $\text{PyCH}_2\text{OCH}_2\text{Py}$  in the erythrocyte ghost mem-

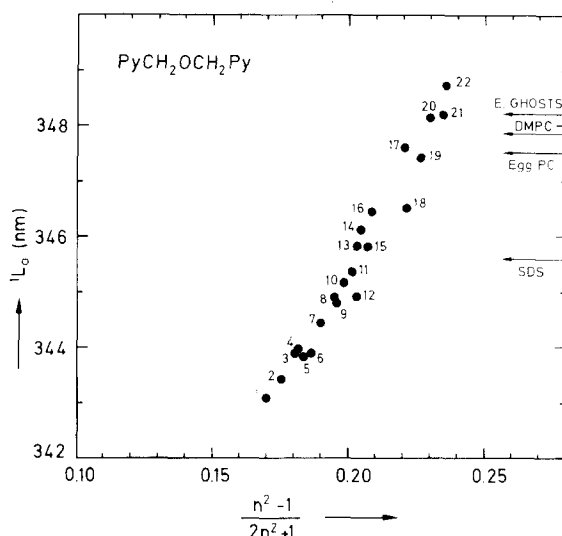


Fig. 6. The energy (in nm) of the first absorption peak of the  $^1L_a$  transition (see Fig. 5) in the spectrum of  $\text{PyCH}_2\text{OCH}_2\text{Py}$  as a function of the solvent polarizability parameter  $(n^2 - 1)/(2n^2 + 1)$ . The transition energies determined with the probe molecule solubilized in a 0.1 M aqueous micellar solution of SDS and in membrane systems of egg PC, DMPC and erythrocyte ghosts (E. Ghosts), are indicated by line segments. For the numbers of the solvents see Experimental.

branes has a surprisingly large value ( $n = 1.513$ ), much larger than the values for hexadecane (1.4346), methanol (1.3298) or water (1.3284), taking solvents that can model a membrane environment containing alkane chains and water. Likewise, large values for the apparent refractive index are observed for the probe surroundings in the other membrane systems,  $n = 1.51$  for multibilayers of DMPC and  $n = 1.50$  for egg PC. Only very polarizable solvents such as pyridine ( $n = 1.5088$ , No. 20 in Fig. 6) or chlorobenzene ( $n = 1.5248$ , No. 21 in Fig. 6) lead to similar shifts in the absorption spectra, but such solvents have a molecular structure that is very different from the constituents of the membrane systems studied here. For  $\text{PyCH}_2\text{OCH}_2\text{Py}$  solubilized in an aqueous micellar solution of SDS, the probe environment is considerably less polarizable, with  $n = 1.43$ , a value even lower than that of liquid paraffin ( $n = 1.4802$ , No. 18), lying between that of hexadecane ( $n = 1.4346$ , No. 15) and  $n$ -hexanol ( $n = 1.4179$ , No. 11) (see the legend to Fig. 6). With the other probe



molecules  $\text{Py}(\text{CH}_2)_3\text{Py}$  and  $\text{PyCH}_2\text{OCH}_3$  similar results are obtained.

The high value for the apparent refractive index,  $n$ , observed here for the probe environment in the membrane systems, can result from the fact that the local density of the probe surroundings is much higher than that encountered in appropriate homogeneous solvents. This would lead to an increase in the polarizability by increasing the electron density. It is of interest to note that it has been concluded from electron density (X-ray) and neutron scattering data that for the erythrocyte ghost membranes the highest local density is found near the head-group region, i.e., near the aqueous interface [36]. This, according to the conclusions drawn above, is the membrane region where the probe molecules are assumed to be localized. In any case these probe molecules in the membrane systems are not located in an environment that contains a large amount of bulk water, as this water, due to its low density, would lead to a reduction of the overall refractive index. This, then, means that the probe molecules are solubilized inside, for example, the erythrocyte ghost membranes, away from the aqueous interface. Similar conclusions were reached in the preceding section on the basis of the fluorescence spectra.

## Conclusion

Probe molecules capable of intramolecular excimer formation, such as  $\text{Py}(\text{CH}_2)_3\text{Py}$  and  $\text{PyCH}_2\text{OCH}_2\text{Py}$ , have been solubilized in erythrocyte ghost membranes. Neither thermotropic phase transitions nor temperature hysteresis effects are observed within the temperature range (0 to 40°C) studied. The viscosity reported by the probes is considerably larger than that of liquid paraffin, with values between 76 cP at 37°C and 570 cP at 5°C, determined by  $\text{Py}(\text{CH}_2)_3\text{Py}$ . The activation energies of intramolecular excimer formation for both dipyrenyl compounds, reflecting the activation energies of diffusion in the medium, also indicate a higher viscosity than that of liquid paraffin.

The two probe molecules,  $\text{Py}(\text{CH}_2)_3\text{Py}$  and  $\text{PyCH}_2\text{OCH}_2\text{Py}$ , display different values for the viscosity. This is interpreted as resulting from a different probe location, the  $\text{PyCH}_2\text{OCH}_2\text{Py}$

molecule, displaying the larger viscosity, being solubilized closer to the membrane/water interface.

From the absorption spectra as well as from the vibrational peak distribution in the fluorescence spectra (the Ham effect) of the probe molecules  $\text{PyCH}_2\text{OCH}_2\text{Py}$  and  $\text{PyCH}_2\text{OCH}_3$ , it is concluded that the direct environment of  $\text{PyCH}_2\text{OCH}_2\text{Py}$  has properties which are clearly different from those of alkane solvents such as hexadecane on the one hand, but also from water, on the other hand. The probe is therefore thought to be completely located inside the membrane, but not in a purely alkane-chain environment, i.e., still close to the polar head-groups. The comparison of the data for membranes with those for a micellar solution of SDS, indicates that the probe molecules in the membranes have their mean location further removed from the water/membrane interface than is the case for the micellar solution. Also the large value for the local polarizability, which is interpreted as a high local density, points to a probe location well inside the membrane, away from the aqueous phase.

## Acknowledgments

Many thanks are due to Mrs. R. Schlegel for assistance with the experiments and for drawing the figures. Dr. T. Jovin and Prof. Dr. A. Stier are thanked for useful comments on the manuscript.

## References

- 1 Zachariasse, K.A. (1978) *Chem. Phys. Lett.* 57 429–432
- 2 Zachariasse, K.A., Kühnle, W. and Weller, A. (1980) *Chem. Phys. Lett.* 73, 6–11
- 3 Georgescauld, D., Desmasez, J.P., Lapouyade, R., Babeau, A., Richard, H. and Winnik, M. (1980) *Photochem. Photobiol.* 31, 539–545
- 4 Galla H.J. and Sackmann E. (1974) *Biochim. Biophys. Acta* 339, 103–115
- 5 Donner, M., Andre, J.C. and Bouchy, M. (1980) *Biochem. Biophys. Res. Commun.* 97, 1183–1191
- 6 Cullis, P.R. and Grathwohl, C. (1977) *Biochim. Biophys. Acta* 471, 213–226
- 7 Glatz, P. (1978) *Anal. Biochem.* 87, 187–194
- 8 Galla, H.J. and Luisetti, J. (1980) *Biochim. Biophys. Acta* 596, 108–117
- 9 Matayoshi, E.D. (1980) *Biochemistry* 19, 3414–3422
- 10 Tanaka, K.I. and Ohnishi, S.I. (1976) *Biochim. Biophys. Acta* 426, 218–231

- 11 Shiga, T., Suda, T. and Maeda, N. (1977) *Biochim. Biophys. Acta* 466, 231–244
- 12 Davis, J.H., Maraviglia, B., Weeks, G. and Godin, D.V. (1979) *Biochim. Biophys. Acta* 550, 362–366
- 13 Verma, S.P. and Wallach, D.F.H. (1976) *Biochim. Biophys. Acta* 436, 307–318
- 14 Gottlieb, M.H. and Eanes, E.D. (1974) *Biochim. Biophys. Acta* 373, 519–522
- 15 Zimmer, G. and Schirmer, H. (1974) *Biochim. Biophys. Acta* 345, 314–320
- 16 Shinitzky, M. and Barenholz, Y. (1978) *Biochim. Biophys. Acta* 515, 367–394
- 17 Kapitza, H.G. and Sackmann, E. (1980) *Biochim. Biophys. Acta* 595, 56–64
- 18 Birks, J.B. (1970) *Photophysics of Aromatic molecules*, ch. 7, Wiley-Interscience, New York
- 19 Flory, P.J. (1969) *Statistical Mechanics of Chain molecules*, ch. 5, Wiley-Interscience, New York
- 20 Dodge, J.T., Mitchell, C. and Hanahan D.J. (1963) *Arch. Biochem. Biophys.* 100, 119–130
- 21 Bodner, B.L., Jackman, L.M. and Morgan, R.S. (1980) *Biochem. Biophys. Res. Commun.* 94, 807–813
- 22 Zachariasse, K.A. and Kühnle, W. (1976) *Z. Physik. Chem.* NF 101, 267–276
- 23 Castellan, A., Desvergne, J.P. and Bouas-Laurent, H. (1979) *Nouv. J. Chim.* 3, 231–238
- 24 Singleton, W.S., Gray, M.S., Brown, M.L. and White, J.L. (1965) *J. Am. Oil Chem. Soc.* 42, 53–56
- 25 Lee, A.G., Birdsall, N.J.M., Metcalfe, J.C., Warren, G.B. and Roberts G.C.K. (1976) *Proc. R. Soc. B* 193, 253–274
- 26 see Seelig, J. and Seelig, A. (1980) *Q. Rev. Biophys.* 13, 19–61
- 27 Nakajima, A. (1973) *Bull. Chem. Soc. Japan* 46, 2602–2604
- 28 Kalyanasundaram, K. and Thomas, J.K. (1977) *J. Am. Chem. Soc.* 99, 2039–2044
- 29 McRae, E.G. (1957) *J. Phys. Chem.* 61, 562–572
- 30 Reichardt, C. (1979) *Angew. Chem. Int. Ed. Engl.* 18, 98–110
- 31 Platt, J.R. (1949) *J. Chem. Phys.* 17, 484–495
- 32 Jaffé, H.H. and Orchin, M. (1962) *Theory and Applications of Ultraviolet Spectroscopy*, Wiley, New York
- 33 Kundt, A. (1878) *Ann. Phys. Chem. N.F.* 4, 34–54
- 34 Mataga, N. and Kubota, T. (1970) *Molecular Interactions and Electronic Spectra*, ch. 8, Dekker, New York
- 35 Bayliss, N.S. (1950) *J. Chem. Phys.* 18, 292–296
- 36 McCaughan, L. and Krimm, S. (1980) *Science* 207, 1481–1483